

Solventless Formation of G-Quartet Complexes Based on Alkali and Alkaline Earth Salts on Au(111)

Chi Zhang, Likun Wang, Lei Xie, Huihui Kong, Qinggang Tan, Liangliang Cai, Qiang Sun, and Wei Xu^{*[a]}

Template cations have been extensively employed in the formation, stabilization and regulation of structural polymorphism of G-quadruplex structures in vitro. However, the direct addition of salts onto solid surfaces, especially under ultra-high-vacuum (UHV) conditions, to explore the feasibility and universality of the formation of G-quartet complexes in a solventless environment has not been reported. By combining UHV-STM imaging and DFT calculations, we have shown that three different G-quartet-M (M: Na/K/Ca) complexes can be obtained on Au(111) using alkali and alkaline earth salts as reactants. We have also identified the driving forces (intra-quartet hydrogen bonding and electrostatic ionic bonding) for the formation of these complexes and quantified the interactions involved. Our results demonstrate a novel route to fabricate G-quartet-related complexes on solid surfaces, providing an alternative feasible way to bring metal elements to surfaces for constructing metal-organic systems.

The formation of G-quadruplex structures in vivo via stacking of G-quartets, which requires template cations to interact with the G-quartets involved, has been proven to be of significance in cellular life processes, and thus has been an intriguing topic for decades.^[1–5] NMR spectroscopy^[6–10] studies have evidenced that in solution, various template cations (normally from different kinds of salts), ranging from monovalent cations (typically alkali cations such as Na⁺, K⁺, Rb⁺) over divalent cations (like alkaline earth cations, namely, Ca²⁺, Sr²⁺, Ba²⁺) to even trivalent lanthanide cations (like La³⁺, Eu³⁺), may play important roles in the formation, stabilization and regulation of structural polymorphism of G-quadruplex structures. Recently, the G-quartet structure has been attractive in the surface science community. For example, several studies demonstrated that G-quartet structures can be induced by Na⁺ and K⁺ cations from salts and adsorb at liquid–solid interfaces, as revealed by ambient scanning tunneling microscopy (STM) with real-space mor-

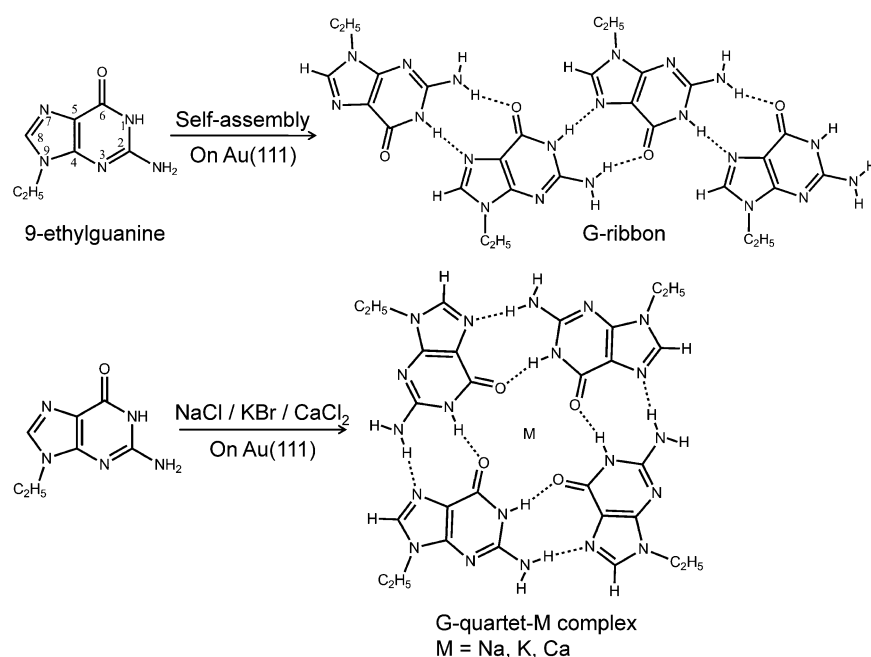
phology.^[11,12] On the other hand, it has been shown by ultra-high-vacuum (UHV) STM that an empty G-quartet network structure^[13,14] can be formed on the Au(111) surface, which could be further stabilized by interacting with K atoms resulting in the formation of a G-quartet-K network structure.^[15] Very recently, an isolated G-quartet-Fe complex was also achieved on an Au(111) surface under well-controlled UHV conditions.^[16] Note that in these cases, the metal atoms were brought onto the surfaces to facilitate the formation of the G-quartet structures and stabilize them. To mimic solution chemistry, it would be of utmost interest to directly add salts onto solid surfaces, especially under UHV conditions, to explore the feasibility and universality of the formation of G-quartet complexes in a solventless environment.

In this study, we have selected the 9-ethylguanine molecule (shortened as 9eG, see Scheme 1) as a guanine (G) analogue because: 1) the possible G/9H to G/7H tautomerization process can be inhibited by modifying the ethyl group to the N9 site;^[17] 2) the 9eG molecule itself forms a G-ribbon structure (see upper panel of Scheme 1 and Figure S1 of the Supporting Information) rather than a G-quartet structure.^[16] With respect to the salts, it was recently reported that NaCl and LiCl thin films grown on solid surfaces can directly interact with organic molecules by providing cations and may then form ionic self-assemblies,^[18–21] which is quite different from their traditional application as insulating layers.^[22–25] Inspired by this, herein, NaCl, KBr and CaCl₂ (typical alkali and alkaline earth salts)^[6–9,11,12] are transferred onto an Au(111) surface to facilitate the subsequent investigation on the formation of possible G-quartet-M complexes (where M denotes Na, K, and Ca, respectively) in such a solventless UHV environment. From the interplay of sub-molecularly resolved UHV-STM imaging and density functional theory (DFT) calculations, we have shown that three sorts of G-quartet-M complexes can indeed be achieved on the Au(111) surface, as schematically depicted in the lower panel of Scheme 1. Charge-density difference and projected density of states (PDOS) analyses qualitatively demonstrate the interactions between M (i.e. Na, K, Ca) and 9eG molecules within G-quartet-M complexes. Furthermore, Bader charge and binding energy analyses allow us to identify the nature of the fundamental interactions involved (that is, electrostatic ionic bonding between positively charged metals and negatively charged oxygen together with intra-quartet hydrogen bonding), and quantify the balance between these two interactions. As a result, we find the stability of G-quartet-M complexes is in the order of G-quartet-Ca > G-quartet-Na > G-quartet-K. These findings demonstrate a novel route to fabricate G-quartet-relat-

[a] C. Zhang,[†] L. Wang,[†] L. Xie, H. Kong, Prof. Dr. Q. Tan, L. Cai, Q. Sun, Prof. Dr. W. Xu
Tongji-Aarhus Joint Research Center for
Nanostructures and Functional Nanomaterials
College of Materials Science and Engineering
Tongji University, Caoan Road 4800
Shanghai 201804 (P. R. China)
E-mail: xuwei@tongji.edu.cn

[†] These authors contributed equally to this work.

Supporting Information for this article is available on the WWW under <http://dx.doi.org/10.1002/cphc.201500301>.



Scheme 1. Schematic illustration of the formation of a G ribbon structure and a G-quartet-M complex on Au(111), where M represents Na, K or Ca.

ed complexes on a solid surface by a solventless method. The direct introduction of salts seems to be an alternative feasible way to bring metal elements to solid surfaces, which could be extended to other systems to investigate molecule-metal interactions in general.

As demonstrated in our previous work, the deposition of 9eG molecules on Au(111) leads to the formation of zigzag ribbon structures (Scheme 1 and Figure S1)^[16,26] rather than G-quartet structures, and besides the intra-quartet hydrogen bonding, a metal center (i.e. Fe in that study) is mandatory for the formation of an isolated G-quartet-Fe complex.^[16] As mentioned above, in this work we focus on the interactions between 9eG

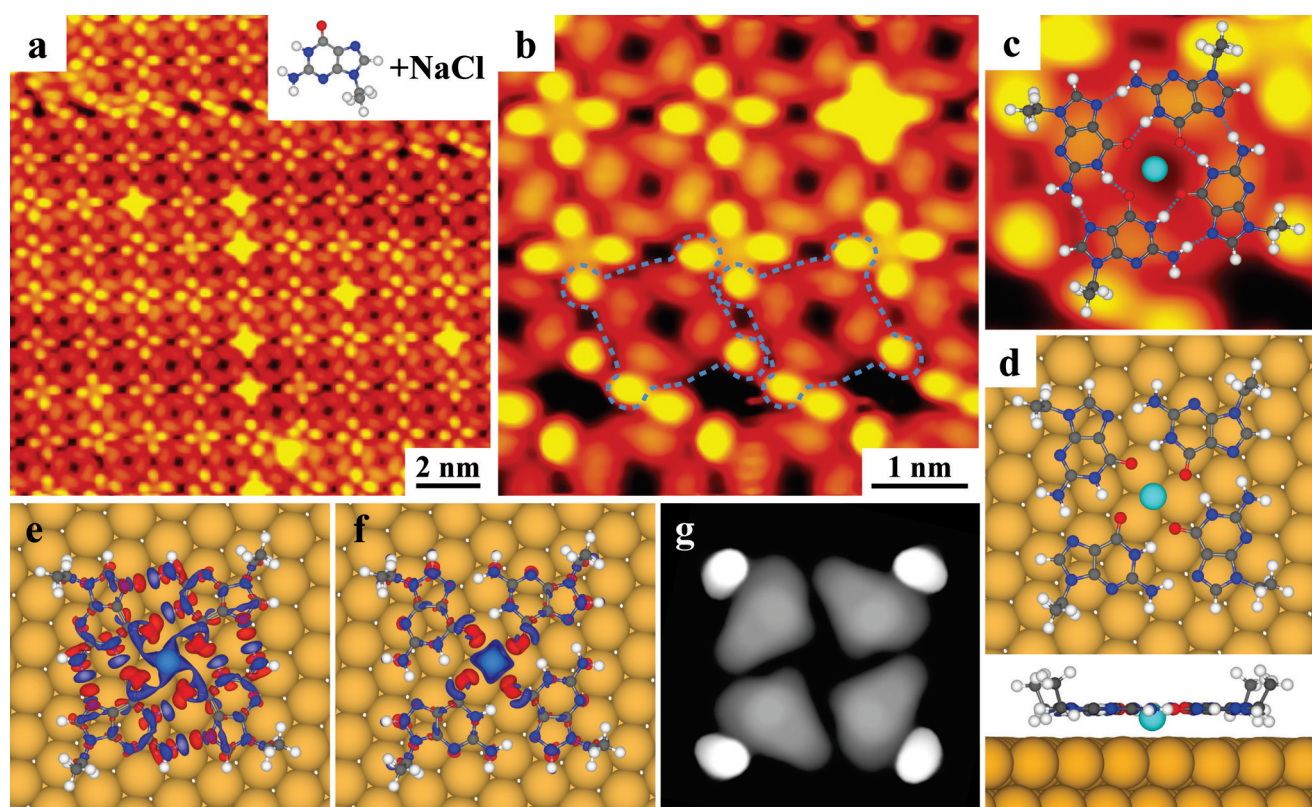


Figure 1. STM image and DFT-optimized structural model showing the formation of a G-quartet-Na complex on Au(111). a) Large-scale STM image showing the formation of the close-packed structure of the G-quartet-Na complex. b) Close-up STM image providing more details of the structure, where two individual G-quartet-Na complexes are depicted by the dashed contours. c) High-resolution STM image of the G-quartet-Na complex superimposed with the DFT-optimized structural model. Scanning conditions: $I_t = 0.9$ nA, $V_t = 2.1$ V. d) Top and side views of the DFT-optimized structural model of the G-quartet-Na complex on Au(111). Au: yellow; H: white; C: gray; N: blue; O: red; Na: azure. e, f) Charge-density-difference maps of the complex showing the intra-quartet hydrogen bonding and the interactions between Na and O [where four 9eG molecules are treated as four individual species in (e) at the isosurface value of 0.0023 eÅ⁻³ and as a whole (G-quartet) in (f) at the isosurface value of 0.0018 eÅ⁻³]. The red and blue isosurfaces indicate charge accumulation and depletion, respectively. g) Simulated STM image of the complex at a bias voltage of 2.1 V.

molecules and different salts on a solid surface. We first added NaCl onto the Au(111) surface held at room temperature (RT), and NaCl islands were observed to grow on the surface (Figure S2), as previously reported.^[27,28] Then, 9eG molecules were deposited onto the NaCl-precovered Au(111) surface and subsequently annealed to ~ 350 K. Interestingly, the formation of ordered close-packed nanostructures (at a coverage of ~ 0.9 ML) composed of G-quartet-Na complexes was successfully achieved, as shown in Figure 1a. A close-up STM image (Figure 1b) allows us to identify the individual G-quartet-Na complexes, as depicted by the dashed contours where the brighter round protrusion and the darker part are attributed to the tilted ethyl group and the guanine moiety, respectively. Note that the central Na can only be visible in the special tip state, as illustrated in Figure S3. The individual complexes bind with neighboring ones via ethyl groups through weak van der Waals (vdW) interactions and mainly form "four-leaf clovers". The bright protrusions in the center of the "four-leaf clovers" may be attributed to the Cl decomposed from NaCl. To get further insight into the complex, we performed detailed DFT calculations based on the high-resolution STM image, as shown in Figure 1c. The energetically most favorable structural model involving the Au(111) substrate is shown in Figure 1d and also superimposed on the STM image with a good agreement (Fig-

ure 1c). Charge-density-difference maps (Figures 1e and 1f) based on the structural model display the intra-quartet hydrogen bonds and the interactions between Na and four O atoms. Furthermore, a corresponding STM image simulation (Figure 1g) was performed at the same bias voltage as the experimental one and a good agreement was also achieved.

We also changed the deposition order of NaCl and the 9eG molecules and found that the formation of the G-quartet-Na complex was not dependent on this. Coverage-dependent experiments were performed as well, where the formation of isolated G-quartet-Na complexes (at a coverage of ~ 0.2 ML) and grid-like nanostructures composed of the complexes (at a coverage of ~ 0.5 ML) was observed owing to the weak vdW interactions among the tilted ethyl groups, as shown in Figure S4. Different ratios of NaCl and 9eG molecules were tried and we found that the formation of the G-quartet-Na complex has nothing to do with the ratios.

To further investigate the universality of using alkali salts for the formation of G-quartet-M complexes and compare other systems with the case of NaCl, we added KBr onto the Au(111) surface held at RT and KBr islands were observed, as shown in Figure S5. The subsequent deposition of 9eG molecules (regardless of the deposition order) and annealing to ~ 350 K, as expected, also resulted in the formation of similar ordered

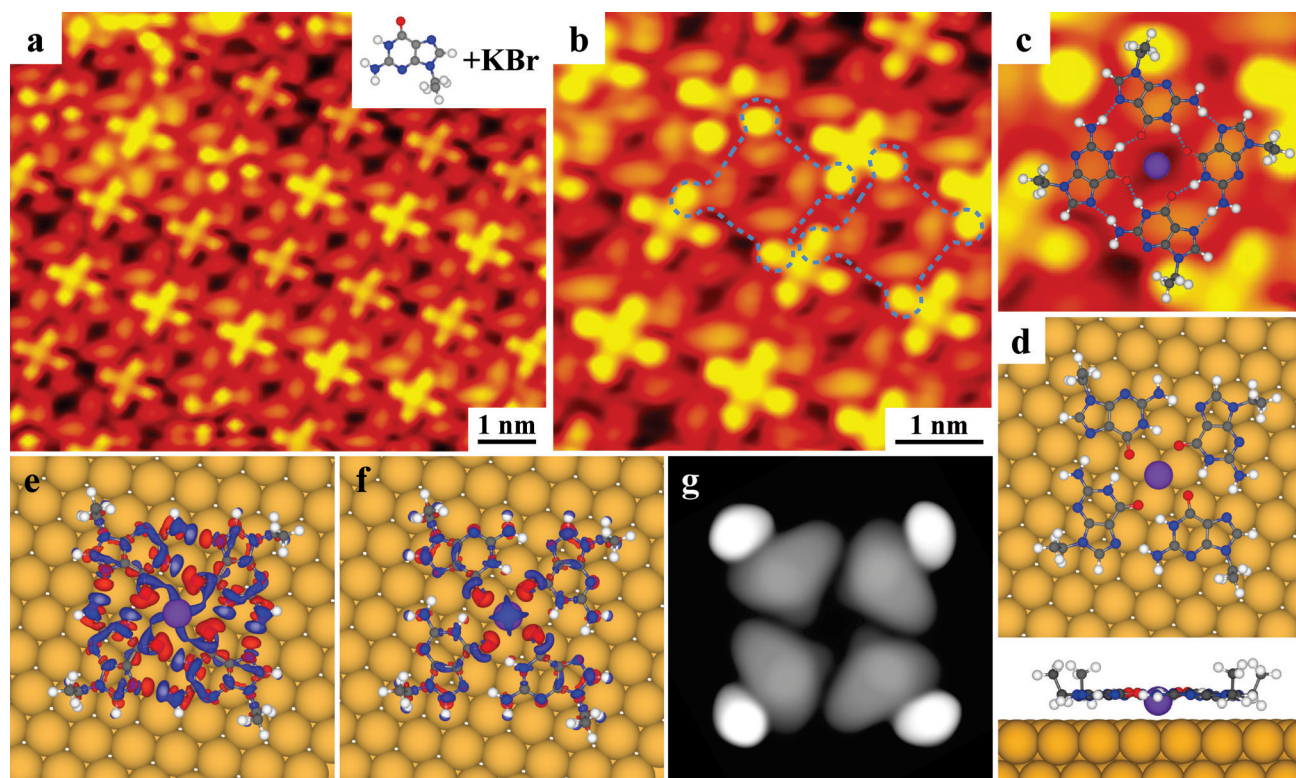


Figure 2. STM image and DFT-optimized structural model showing the formation of a G-quartet-K complex on Au(111). a) Large-scale STM image showing the formation of the close-packed structure of the G-quartet-K complex. b) Close-up STM image providing more details of the structure, where two individual G-quartet-K complexes are depicted by the dashed contours. c) High-resolution STM image of the G-quartet-K complex superimposed with the DFT-optimized structural model. Scanning conditions: $I_t = 0.9$ nA, $V_t = 2.1$ V. d) Top and side views of the DFT-optimized structural model of the G-quartet-K complex on Au(111). Au: yellow; H: white; C: gray; N: blue; O: red; K: purple. e, f) Charge-density-difference maps of the complex showing the intra-quartet hydrogen bonding and the interactions between K and O [where four 9eG molecules are treated as four individual species in (e) at the isosurface value of 0.0017 eÅ⁻³ and as a whole (G-quartet) in (f) at the isosurface value of 0.0012 eÅ⁻³]. The red and blue isosurfaces indicate charge accumulation and depletion, respectively. g) Simulated STM image of the complex at a bias voltage of 2.1 V.

close-packed nanostructures composed of G-quartet-K complexes, as shown in Figure 2a. The individual G-quartet-K complexes can be identified from the close-up STM image (Figure 2b), as depicted by the dashed contours, and such complexes bind with neighboring ones via ethyl groups through weak vdW interactions as well. Based on the high-resolution STM image, as shown in Figure 2c, we performed detailed DFT calculations, and the energetically most favorable structural model involving the substrate is shown in Figure 2d and also superimposed on the STM image with a good agreement (Figure 2c). Charge-density-difference maps (see Figures 2e and 2f) display the intra-quartet hydrogen bonds and the interactions between K and four O atoms. A simulated STM image was obtained, as shown in Figure 2g, and is also in accordance with the experimental one.

To move a step forward and extend the generality of the salts to different main-group elements, CaCl_2 —a typical divalent alkaline earth salt—was added onto the Au(111) surface held at RT, and CaCl_2 islands were observed, as shown in Figure S6. After subsequent deposition of 9eG molecules on the Au(111) substrate (regardless of the deposition sequence) and further annealing to ~ 350 K, ordered grid-like nanostructures (like in the case of G-quartet-Fe)^[16] composed of G-quartet-Ca

complexes were successfully formed, as shown in Figure 3a. A close-up STM image (Figure 3b) allows us to identify the individual G-quartet-Ca complexes, as depicted by the dashed contours, and such complexes bind with neighboring ones via ethyl groups as well. Based on the high-resolution STM image (Figure 3c), we performed detailed DFT calculations and the energetically most favorable structural model involving the substrate is shown in Figure 3d and also superimposed on the STM image with a good agreement (Figure 3c). Charge-density-difference maps (Figures 3e and 3f) illustrate the inter-quartet hydrogen bonds and the interactions between Ca and four O atoms. A simulated STM image was obtained, as shown in Figure 3g, and is also in accordance with the experimental one.

To gain a deeper insight into the interactions between metal atoms and 9eG molecules within G-quartet-M complexes, the PDOS of the metal atoms (i.e. Na, K and Ca) in the gas phase on the s and p orbitals of the metal atoms and the PDOS of the G-quartet-M complexes on Au(111) on the s and p orbitals of the metal atom and four neighboring O atoms were calculated as plotted in Figure 4. By comparing these three rows we could identify that the expected charge transfers from the metal atoms to the four O atoms took place, as hybridization

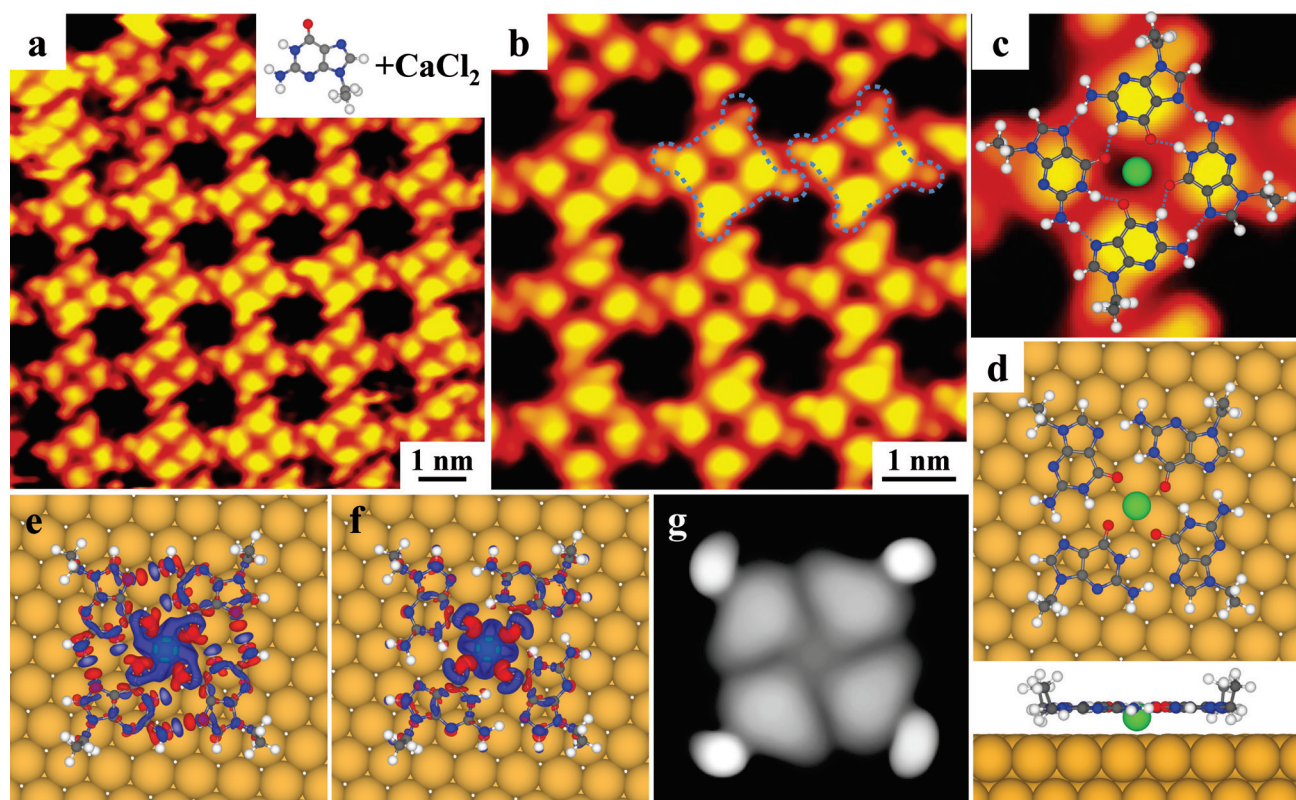


Figure 3. STM image and DFT-optimized structural model showing the formation of a G-quartet-Ca complex on Au(111). a) Large-scale STM image showing the formation of the grid-like structures of the G-quartet-Ca complex. b) Close-up STM image providing more details of the structure, where two individual G-quartet-Ca complexes are depicted by the dashed contours. c) High-resolution STM image of the G-quartet-Ca complex superimposed with the DFT-optimized structural model. Scanning conditions: $I_t = 1.1$ nA, $V_t = 2.1$ V. d) Top and side views of the DFT-optimized structural model of the G-quartet-Ca complex on Au(111). Au: yellow; H: white; C: gray; N: blue; O: red; Ca: green. e, f) Charge-density-difference maps of the complex showing the intra-quartet hydrogen bonding and the interactions between Ca and O [where four 9eG molecules are treated as four individual species in (e) at the isosurface value of $0.0025 \text{ e}\text{\AA}^{-3}$ and as a whole (G-quartet) in (f) at the isosurface value of $0.002 \text{ e}\text{\AA}^{-3}$]. The red and blue isosurfaces indicate charge accumulation and depletion, respectively. g) Simulated STM image of the complex at a bias voltage of 2.1 V.

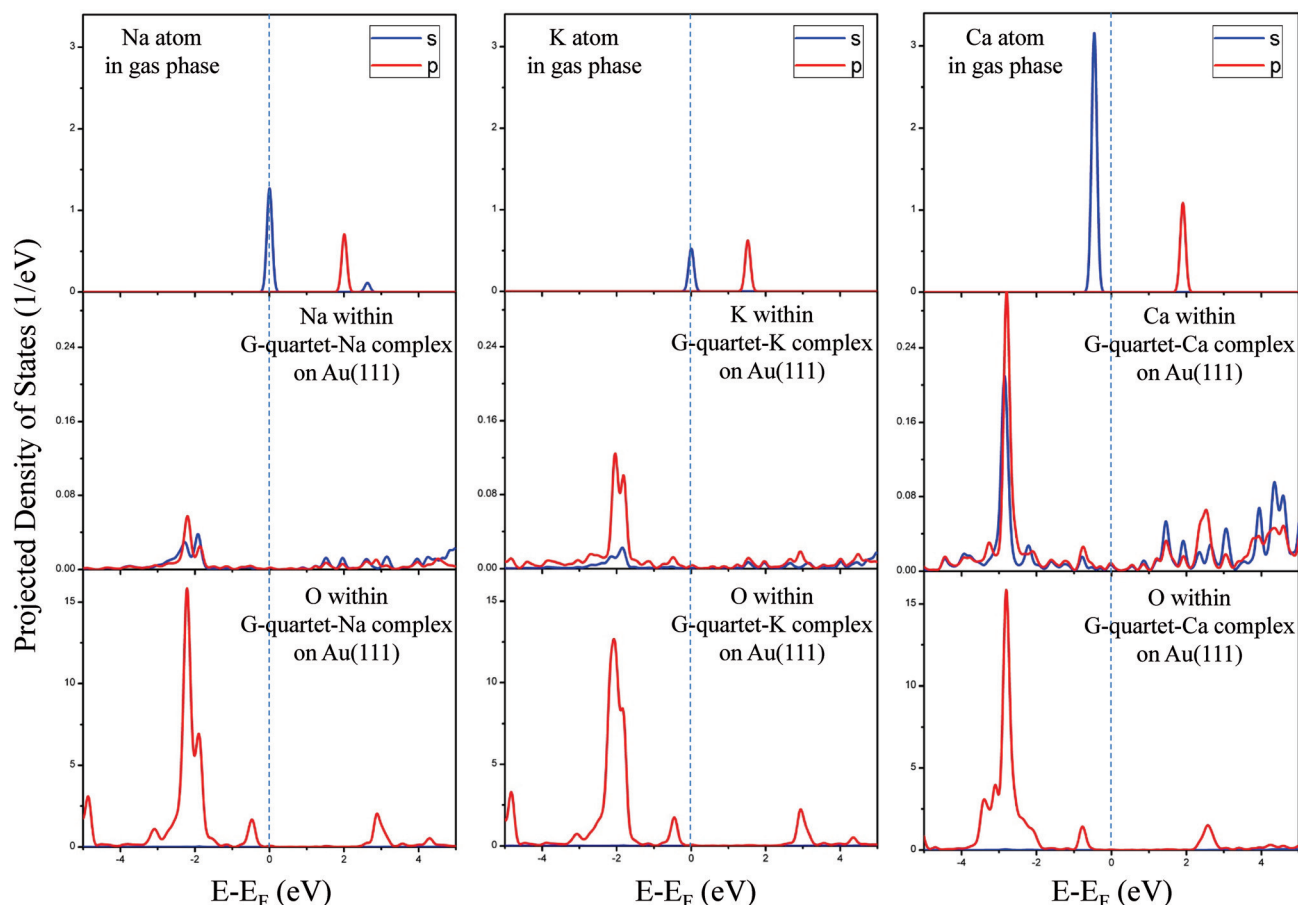


Figure 4. Top: Calculated projected density of states (PDOS) (in eV with respect to the Fermi energy E_F) of the metal atoms in the gas phase on the s and p orbitals of the metal atoms. Middle and bottom: Calculated PDOS of the G-quartet-M complexes on Au(111) on the s and p orbitals of the metal atoms and the four neighboring O atoms, respectively. The Fermi level is marked as a dashed vertical line in each panel.

peaks of the p orbitals of metal atoms and the O atoms can be observed (at about -2.2 eV for G-quartet-Na, -2.0 eV for G-quartet-K, and -2.8 eV for G-quartet-Ca), and the density of states of the central metal atoms are different from those of the neutral ones in the gas phase (as the s orbitals move from E_F to -2.2 eV for Na, E_F to -2.0 eV for K, and -0.46 eV to -2.8 eV for Ca), which is also confirmed by the charge-density-difference maps displayed above.

From the above analyses of the PDOS and the charge-density-difference maps we could qualitatively confirm that the charge transfers occurred from the metal centers to the O atoms within the G-quartet-M complexes. A further step would be to identify the nature of the interactions and quantify the driving forces for the formation of G-quartet-M complexes. We then performed a Bader charge analysis based on DFT calculations, as shown in Table 1. The Bader charge analysis quantitatively indicates that: 1) in the empty G-quartet charge is accumulated on the O atoms related to the intra-quartet hydrogen bonds;^[13] 2) within the G-quartet-M complexes on Au(111), all three metal centers are positively charged (Na is in a $+0.87$ charged state, K is in a $+0.84$ charged state, and Ca is in a $+1.58$ charged state); 3) the four O atoms are all more negatively charged after interacting with the metal centers; and

Table 1. Bader charge analysis quantitatively showing the charged states of the metal and O atoms in different environments.

	Na/K/Ca	O
9eG in the gas phase	–	-1.07
9eG on Au(111)	–	-1.05
G-quartet in the gas phase	–	-1.10
G-quartet on Au(111)	–	-1.15
G-quartet-Na in the gas phase	0.88	-1.17
G-quartet-Na on Au(111)	0.87	-1.15
G-quartet-K in the gas phase	0.87	-1.20
G-quartet-K on Au(111)	0.84	-1.18
G-quartet-Ca in the gas phase	1.57	-1.24
G-quartet-Ca on Au(111)	1.58	-1.21

4) the Au(111) substrate may partly screen such interactions resulting in the overall neutrality of the whole system.^[19,20,29,30]

Note that similar systems based on tetracyanoquinodimethane (TCNQ) and carboxylate-functionalized molecules interacting with NaCl/LiCl on Au(111) have also been reported, the XPS data directly evidencing that charge transfers occur between Na/Li and the organic molecules resulting in the formation of $\text{Na}^+[\text{TCNQ}]^-/\text{Li}^+[\text{TCNQ}]^-$, and dominantly $\text{Na}^+[\text{TPA}]^{2-}/$

Table 2. Binding energies of three different G-quartet-M complexes in the gas phase with the corresponding structural models.

	G-quartet-Na	G-quartet-K	G-quartet-Ca
structural model			
hydrogen bonding [eV]	3.95	3.96	3.95
electrostatic ionic bonding [eV]	2.32	1.81	2.70
total binding energy [eV]	6.27	5.77	6.65

Na⁺[BTA]⁴⁻, ionic layers.^[18–21] To compare this with our case, we also performed a Bader charge analysis on one of the above systems,^[18] that is, a Na-(TCNQ)₄ structural motif on Au(111) (Figure S7), where Na is also calculated to be in a +0.87 charged state, which is very similar to the case of the G-quartet-Na complex. Thus, we can convincingly draw the conclusion that the interactions between metal centers and O atoms within G-quartet-M complexes should be attributed to electrostatic ionic bonding.^[29,30]

To finally quantify the different interactions (i.e. intra-quartet hydrogen bonding and electrostatic ionic bonding) involved within these complexes, analyses of the binding energies of the complexes were performed based on the gas-phase optimized structural models, as depicted in Table 2. From the calculations we could identify that the intra-quartet hydrogen bonding within these complexes contributes almost the same, about 3.95 eV (including the corresponding vdW interactions). The electrostatic ionic bonding (including the corresponding vdW interactions) between the metal centers and the O atoms were calculated to be 2.32, 1.81 and 2.70 eV for G-quartet-Na, G-quartet-K and G-quartet-Ca, respectively. As a result, among these complexes, the G-quartet-Ca complex is the most stable one with the highest binding energy of 6.65 eV. It is also noticeable from the structural models that only K is bound above the molecular plane, which may account for a lower electrostatic ionic and the final total binding energy (5.77 eV), as compared to the case of the G-quartet-Na complex (6.27 eV).

In conclusion, by combining high-resolution STM and DFT calculations, we presented the formation of three different G-quartet-M complexes on Au(111) using alkali and alkaline earth salts as reactants in a solventless UHV environment. From the detailed DFT calculations we identified that the driving forces for the formation of G-quartet-M complexes are the cooperative effects of intra-quartet hydrogen bonding and electrostatic ionic bonding between the metal center and the oxygen atoms; we further quantified the interactions involved. These findings may serve as a prototypical system to investigate the on-surface self-assembly or in situ chemical reaction process by the direct introduction of salts, instead of metal atoms, and may also open a promising way to effectively fabricate metal-organic complexes or nanostructures on solid surfaces.

Acknowledgements

The authors acknowledge financial support from the National Natural Science Foundation of China (21103128, 21473123), the

Research Fund for the Doctoral Program of Higher Education of China (20120072110045). Prof. Flemming Besenbacher is acknowledged for fruitful discussions.

Keywords: density functional theory · electrostatic ionic interactions · G-quartet · salts · scanning tunneling microscopy

- [1] S. Kumari, A. Bugaut, J. L. Huppert, S. Balasubramanian, *Nat. Chem. Biol.* **2007**, *3*, 218–221.
- [2] G. Biffi, D. Tannahill, J. McCafferty, S. Balasubramanian, *Nat. Chem.* **2013**, *5*, 182–186.
- [3] M. L. Bochman, K. Paeschke, V. A. Zakian, *Nat. Rev. Genet.* **2012**, *13*, 770–780.
- [4] K. I. McLuckie, M. Di Antonio, H. Zecchini, J. Xian, C. Caldas, B. F. Krippeendorff, D. Tannahill, C. Lowe, S. Balasubramanian, *J. Am. Chem. Soc.* **2013**, *135*, 9640–9643.
- [5] J. R. Williamson, *Annu. Rev. Biophys. Biomol. Struct.* **1994**, *23*, 703–730.
- [6] R. Ida, G. Wu, *J. Am. Chem. Soc.* **2008**, *130*, 3590–3602.
- [7] I. C. M. Kwan, A. Wong, Y. M. She, M. E. Smith, G. Wu, *Chem. Commun.* **2008**, 682–684.
- [8] I. C. M. Kwan, X. Mo, G. Wu, *J. Am. Chem. Soc.* **2007**, *129*, 2398–2407.
- [9] K. Snoussi, B. Halle, *Biochemistry* **2008**, *47*, 12219–12229.
- [10] I. C. M. Kwan, Y. M. She, G. Wu, *Chem. Commun.* **2007**, 4286–4288.
- [11] A. Ciesielski, S. Lena, S. Masiero, G. P. Spada, P. Samori, *Angew. Chem. Int. Ed.* **2010**, *49*, 1963–1966.
- [12] D. González-Rodríguez, P. G. Janssen, R. Martín-Rapún, I. D. Cat, S. De Feyter, A. P. Schenning, E. W. Meijer, *J. Am. Chem. Soc.* **2009**, *132*, 4710–4719.
- [13] R. Otero, M. Schöck, L. M. Molina, E. Lægsgaard, I. Stensgaard, B. Hammer, F. Besenbacher, *Angew. Chem. Int. Ed.* **2005**, *44*, 2270–2275.
- [14] W. Xu, R. E. Kelly, H. Gersen, E. Lægsgaard, I. Stensgaard, L. N. Kantorovich, F. Besenbacher, *Small* **2009**, *5*, 1952–1956.
- [15] W. Xu, Q. Tan, M. Yu, Q. Sun, H. Kong, E. Lægsgaard, I. Stensgaard, J. Kjems, J. Wang, C. Wang, F. Besenbacher, *Chem. Commun.* **2013**, *49*, 7210–7212.
- [16] L. Wang, H. Kong, C. Zhang, Q. Sun, L. Cai, Q. Tan, F. Besenbacher, W. Xu, *ACS nano* **2014**, *8*, 11799–11805.
- [17] H. Kong, Q. Sun, L. Wang, Q. Tan, C. Zhang, K. Sheng, W. Xu, *ACS nano* **2014**, *8*, 1804–1808.
- [18] C. Wäckerlin, C. Iacovita, D. Chylarecka, P. Fesser, T. A. Jung, N. Ballav, *Chem. Commun.* **2011**, *47*, 9146–9148.
- [19] D. Skomski, S. Abb, S. L. Tait, *J. Am. Chem. Soc.* **2012**, *134*, 14165–14171.
- [20] D. Skomski, S. L. Tait, *J. Phys. Chem. C* **2013**, *117*, 2959–2965.
- [21] T. K. Shimizu, J. Jung, H. Imada, Y. Kim, *Angew. Chem. Int. Ed.* **2014**, *53*, 13729–13733.
- [22] J. Repp, G. Meyer, S. M. Stojković, A. Gourdon, C. Joachim, *Phys. Rev. Lett.* **2005**, *94*, 026803.
- [23] P. Liljeroth, J. Repp, G. Meyer, *Science* **2007**, *317*, 1203–1206.
- [24] B. Such, G. Goryl, S. Godlewski, J. J. Kolodziej, M. Szymanski, *Nanotechnology* **2008**, *19*, 475705.
- [25] J. Repp, G. Meyer, S. Paavilainen, F. E. Olsson, M. Persson, *Science* **2006**, *312*, 1196–1199.
- [26] W. Xu, J. G. Wang, M. F. Jacobsen, M. Mura, M. Yu, R. E. A. Kelly, Q. Meng, E. Lægsgaard, I. Stensgaard, T. R. Linderöth, J. Kjems, L. N. Kantorovich, K. V. Gothelf, F. Besenbacher, *Angew. Chem. Int. Ed.* **2010**, *49*, 9373–9377; *Angew. Chem.* **2010**, *122*, 9563–9567.

- [27] K. Lauwaet, K. Schouteden, E. Janssens, C. Van Haesendonck, P. Lievens, M. I. Trioni, L. Giordano, G. Pacchioni, *Phys. Rev. B* **2012**, *85*, 245440.
- [28] C. Bombis, N. Kalashnyk, W. Xu, E. Lægsgaard, F. Besenbacher, T. R. Linderoth, *Small* **2009**, *5*, 2177–2182.
- [29] S. Stepanow, R. Ohmann, F. Leroy, N. Lin, T. Strunskus, C. Woll, K. Kern, *ACS nano* **2010**, *4*, 1813–1820.
- [30] N. Abdurakhmanova, A. Floris, T. C. Tseng, A. Comisso, S. Stepanow, A. De Vita, K. Kern, *Nat. Commun.* **2012**, *3*, 940.

Received: April 13, 2015

Published online on April 27, 2015